

MESOSCALE AIR POLLUTION DISPERSION MODELS—II. LAGRANGIAN PUFF MODEL AND COMPARISON WITH EULERIAN GRID MODEL

N. D. VAN EGMOND and H. KESSEBOOM

National Institute of Public Health, Bilthoven, The Netherlands

(First received 4 December 1981 and in final form 26 April 1982)

Abstract—A Lagrangian PUFF model has been developed to describe the mesoscale SO₂ concentration fields for a 400 km side square containing The Netherlands. The model is vertically stratified in three atmospheric layers. It can describe the major concentration variability in space and time. By application of a plume segment approach the spatial resolution of 15 km can be increased to about 1 km; on these smaller geographic scales the model is compatible with the conventional Gaussian plume model. The model performance is satisfying: spatial correlations are in the order of 0.7 and probably can be increased by updating the emission inventory. In mesoscale applications, the Lagrangian PUFF model has a higher computational efficiency than the comparable GRID model.

1. INTRODUCTION

For the quantitative interpretation of the measurement results of the Dutch national air pollution monitoring network two retrospective models were developed. Based on the same treatment of meteorology, pollutant transport over the 400 km × 400 km square around The Netherlands is described by both an Eulerian GRID and a Lagrangian PUFF model. The GRID model, with its potential capacity of handling several reacting pollutant species, was described in the preceding paper (van Egmond and Kesseboom, 1983). Referring to the outline of the meteorological treatment given there the Lagrangian PUFF model will be described together with its specific advantages with respect to spatial resolution and computational efficiency.

2. EMISSIONS

The SO₂-emissions for the PUFF model are based on the same inventarisation as for the GRID model (TNO, 1979). The 15 km × 15 km grid cell-area sources were converted to initial Gaussian puffs with $2 \times \sigma_{ro}$ diameters of 15 km. For extended source areas several adjacent grid cells are combined into larger emission puffs. Effective plume heights for these areas are computed as a mean of the individual source heights, weighted according to the emission strengths. Within The Netherlands a number of point sources are taken into account by generating small initial puffs with diameters of 10 m. All puffs consist of both an upper and a lower level to account for emission and/or transport in two separate atmospheric layers. The puffs are generated at time intervals such that constant interpuff-distances are obtained over the field.

3. METEOROLOGY

The PUFF model is based on the same meteorology as the GRID model. Vertical stratification is given by a surface, a mixing and a reservoir layer. From 10-m windspeed data and solar radiation flux, the Obukhov length L and friction velocity u_* are derived. These stability parameters then lead to the dry deposition flux over the surface layer and the resulting vertical SO₂ concentration profile. Within the mixing layer the vertical concentration profile is assumed to be Gaussian. The increase in vertical plume dimensions is described in the usual way by the empirical function

$$\sigma_z(x) = ax^b$$

where a and b depend on the Pasquill stability class as given by Table 1. The stability is derived for every hour from the Obukhov length L and roughness length $z_o = 0.05$ m according to the scheme given by Golder (1972).

Table 1. Coefficient a and exponent b in $\sigma_z(x) = ax^b$ as a function of Pasquill stability class

Pasquill class	a	b
A	0.28	0.90
B	0.23	0.85
C	0.22	0.80
D	0.20	0.76
E	0.15	0.73
F	0.12	0.67

3.1. Advection and dispersion

The horizontal concentration distribution in the puff is only dependent on the distance r to the puff

centre:

$$C(r) = f \frac{M}{2\pi\sigma_r^2 h} \exp(-r^2/2\sigma_r^2), \quad (1)$$

where M is the mass represented by the reservoir or mixing layer part of the puff for time step Δt and emission Q (kg s^{-1}), obtained as $M = Q\Delta t$; h is the height of the reservoir (or mixing) layer; σ_r is the horizontal extend of the puff; f is a factor to take the vertical concentration profile in the mixing layer into account; in the reservoir layer the distribution is fully two-dimensional and $f = 1$.

The puffs are generated with an initial diameter σ_{r0} and advected over the field according to the local u, v -wind components of the layer in which the pollutant mass is the largest. The time steps at which the puffs are generated are chosen such that the interpuff distances have a preset value; in the present applications a value of 10 km is used. At low wind speeds puffs are generated at least once per hour. During the first hour the time step of advection equals that of puff generation, which in most cases is less than one hour. As the puff growth due to dispersion is most significant during the first hour of transport, this growth can be calculated from

$$\sigma_{rt+\Delta t}^2 = \sigma_{rt}^2 + 2K_H\Delta t. \quad (2)$$

The apparent horizontal diffusivity K_H is time dependent and given by

$$K_H(t) = \overline{v_m^2} \int_0^t R_L(\tau) d\tau, \quad (3)$$

where $\overline{v_m^2}$ is the (Eulerian) cross wind turbulence (hourly average) derived from the measured standard deviation of wind direction and from wind speed (minute values).

$R_L(\tau) = e^{-\tau/t_L}$, the Lagrangian correlation function with time scale t_L .

For every puff, the value of $K_H(t)$ is evaluated from (3) at every time step and the puff diameter increased according to (2), as illustrated by Fig. 1. After the first hour the advection time step is set to one hour, in accordance with the time resolution of the wind fields.

To compare this numerical procedure to the usual Gaussian plume model the time dependent plume

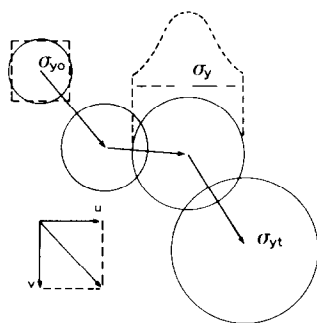


Fig. 1. Advection and dispersion of puffs.

width σ_r is written in analytical form by application of Taylor's theorem (Csanady, 1973)

$$\sigma_r^2(t) = 2\overline{v_m^2} \int_0^t \int_0^{t'} R_L(\tau) d\tau dt', \quad (4)$$

which when $R_L(\tau) = e^{-\tau/t_L}$ gives

$$\sigma_r^2(t) = 2\overline{v_m^2} t_L^2 (t/t_L - 1 + e^{-t/t_L}). \quad (5)$$

In Table 2 the plume width according to (5) and $\sigma_y = 0.371x^{0.87}$ at Pasquill stability B and 16 m wind speed of 4 m s^{-1} (4.7 m s^{-1} at 50 m height) is given for downwind distances between 1 and 50 km. Herein the Lagrangian time scale t_L is set to 40 min to obtain good agreement between puff growth [Equations (2) and (3)] and the Gaussian plume model.

Table 2. σ_r according to Equation (5) and $\sigma_y = 0.371x^{0.87}$ at Pasquill B, 4 m s^{-1}

Distance x (km)	time t (min)	σ_r^* (m)	σ_y (Gauss. Pl. Mod.) (m)
1.4	5	203	196
5.6	20	767	651
17.0	60	2000	1705
34.0	120	3366	3107
51.0	180	4408	4415

* Equation (5).

Vertical stratification is obtained by considering separate masses for reservoir and mixing layer within every puff. During fumigation the mixing height rises and mass is transported proportionally from the reservoir to the mixing layer, as illustrated by Fig. 2. Within the mixing layer the vertical concentration distribution is assumed to be Gaussian. The ground level concentration is found by introducing the factor f in (1).

For the mixing layer:

$$f = \frac{2h}{\sqrt{2\pi}\sigma_z} \left[\exp\left(-\frac{1H^2}{2\sigma_z^2}\right) + \exp\left(-\frac{1(2h-H)^2}{2\sigma_z^2}\right) + \exp\left(-\frac{1(2h+H)^2}{2\sigma_z^2}\right) \right] \quad (6)$$

where h is mixing height, H is the effective source height and σ_z is the vertical standard deviation and given by $\sigma_z = ax^b$, where a and b are given in Table 1 for the Pasquill stability classes, to be derived from

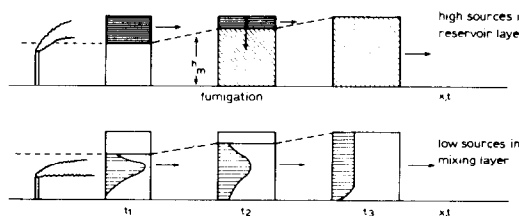


Fig. 2. Vertical stratification of pollution in reservoir and mixing layer and downward transport during fumigation.

Obukhov length and roughness length according to Golder (1972).

At larger distances, f is limited to the ratio between the concentrations at 4 and 50 m height. This ratio is derived from the surface layer parameters under the assumption of a height independent SO₂ flux.

The puffs finally are projected on a grid from which concentration fields can be plotted. By varying the grid-length of this grid, a wide range of spatial resolutions can be obtained. Apart from the mesoscale concentration fields, with a grid length $\Delta x = 15$ km, detailed concentration patterns within relevant areas can be obtained ($\Delta x = 3$ km). However this implies a wide range of ratios between grid-lengths and puff-diameters, resulting in irregularities in the concentration fields or in computational inefficiency. For this reason the puffs will be treated as plume-segments in cases where the puff-diameters are small compared to the grid-length, as illustrated in Fig. 3. The plume segment then is given by a number of pseudo-puffs which are generated along the plume-direction vector; this vector is identical to the wind vector at the time of the puff release and associated with the puff during the total transport time. The pseudo-puff approach avoids discontinuities at the intersection of two adjacent segments.

The increase of pseudo-puff dimensions along the plume direction vector is accounted for by the procedure given by (2) and (3). The dependence of $\overline{v_m^2}$ on averaging time at time steps less than 1 h is neglected.

An example of the application of the PUFF model

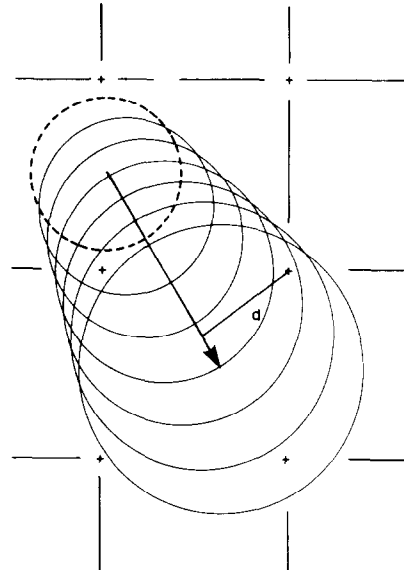


Fig. 3. Superposition of pseudo-puffs on plume segment vector; the initial puff is given by a dashed line.

both for the 400 km square area and the detailed 80 km square urban-industrial subarea in the western part of Holland, is given in Fig. 4. In the map of this subarea, the plumes of the individual emissions of the Rotterdam-Rijnmond industrial area appear superimposed on the mesoscale plumes, which appear on the 400 km × 400 km map.

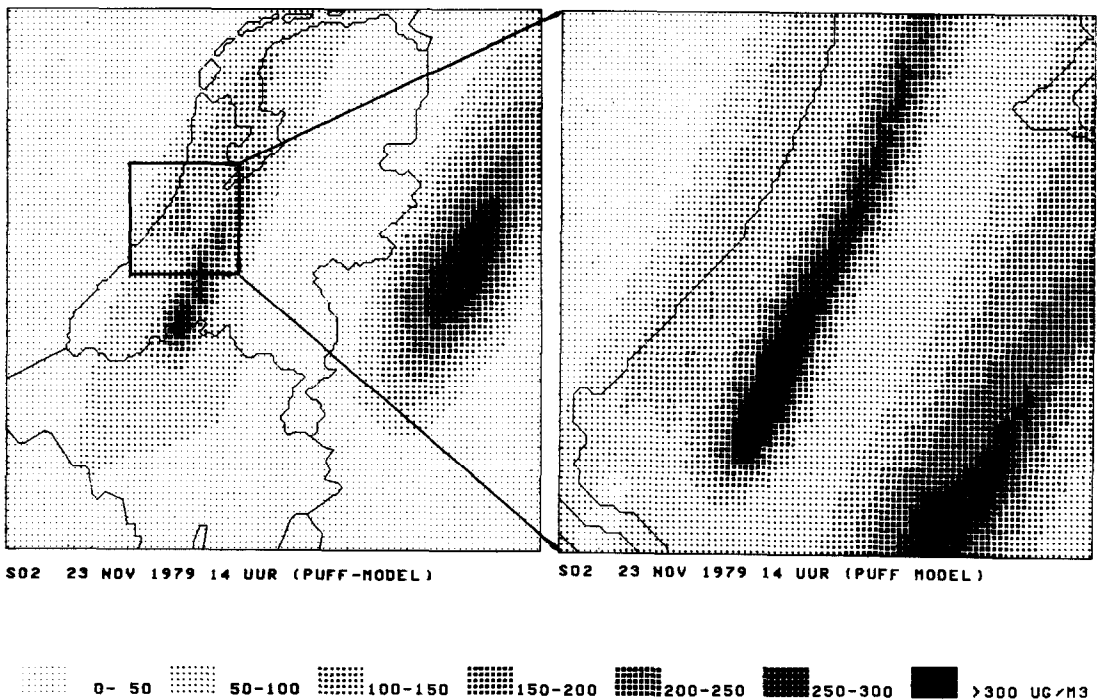


Fig. 4. Modelled SO₂ concentration fields for the 400 km × 400 km surroundings of The Netherlands and for the 80 km × 80 km subarea with increased spatial resolution.

4. COMPUTATIONAL ASPECTS

The PUFF model is designed for operational application on a mini-computer configuration and implemented on a HP 1000 F system under RTE-IV. The model is embedded in the data-handling and information system of the National Air Pollution Monitoring Network. The program PUFF is not segmented and requires 52 K bytes memory. For every puff the following 10 parameters are stored:

- x , position;
- y , position;
- σ_r , standard deviation of puff;
- t , total time of travel;
- f , fraction of mixing layer concentration affecting ground level;
- M_r , mass in reservoir layer;
- M_m , mass in mixing layer;
- x , component plume segment sector (wind vector at time of emission);
- y , component plume segment vector
- H , effective height of initial emission.

With about 5000 puffs a total array of about 100 K is required to store these 10 parameters. With about 20 K for additional arrays the total required memory capacity is about $52 + 100 + 20 = 172$ K bytes. In order to stay within the limits of available memory capacity the program keeps track of the total number of puffs. When the maximum number of 5000 puffs is exceeded the program stops and might be rerun with an increased interpuff distance. At the present applications interpuff distances of 10 km did not result in overflow of the storage area for puff parameters. In special cases or in applications of the model on a desktop computer, puff parameters might be stored on disc and efficiently handled by buffered input and output.

Apart from a constant computation time required for the evaluation of meteorological parameters at every hour of simulation, the computation in the PUFF model is proportional to the number of puffs. As the interpuff distances are constant (about 10 km) the computation time is then proportional to the number of sources, as presented in Fig. 5. For comparison the time required for 1-h simulation by the GRID model (van Egmond and Kesseboom, 1983) is given in the same figure. With the present number of 148 sources the PUFF model is more efficient than the GRID model. In urban applications, where the number of (low or high) sources equals the number of grid cells = $32 \times 32 = 1024$, the PUFF model will be less efficient than the GRID model with the same spatial resolution.

5. SENSITIVITY ANALYSIS; COMPARISON WITH THE GRID MODEL

The sensitivity of the PUFF model to many of the meteorological parameters is nearly the same as in the GRID model. Due to the essentially different treatment of horizontal plume growth an exception is given by horizontal dispersion.

Horizontal dispersion was enhanced by increasing the r.m.s. turbulence with an arbitrary factor $\sqrt{20}$. This resulted in a decrease of the concentration maximum by 28% at 200 km downwind of the 15-km source area.

Horizontal wind shear dispersion is modelled improperly by the PUFF model; both mixing and reservoir layer pollution are handled by the same puffs, thus having the same geographical positions. When during fumigation the mixing layer mass becomes

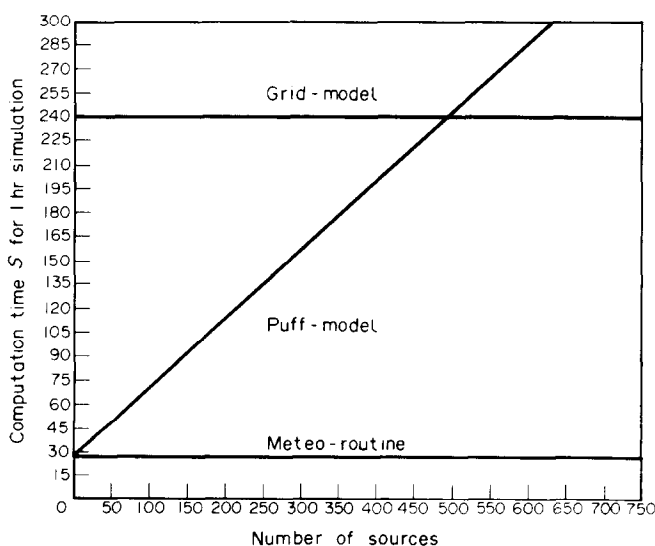


Fig. 5. Computation times for the models PUFF and GRID as a function of the number of sources.

larger than the reservoir layer mass, the transport direction is then deduced from the mixing layer wind field but the horizontal extent of the puff is maintained, so that wind shear dispersion is eliminated. In the GRID model the reservoir layer mass is transported downwards to the mixing layer, where it is instantaneously mixed and transported according to the mixing layer wind. This results in a realistic modelling of wind shear dispersion. This difference in performance between PUFF and GRID model is illustrated by Fig. 6.

Mass consistency was maintained within 2%, as evaluated from an advected isolated puff, representing 1 h of emission. These small fluctuations in mass result from the positioning of the puffs with respect to the grid on which the puffs are projected.

6. CASE STUDY AND MODEL PERFORMANCE

The performance of the PUFF model is illustrated by means of a case study of 20 and 21 February 1980. The air pollution levels in this period were not exceptional but representative for the anti-cyclonic south-east circulations which generally give rise to increased SO_2 concentrations.

A high pressure system over the U.S.S.R. maintained a south-easterly flow of $3\text{--}5\text{ m s}^{-1}$ over the model area. During the night temperatures of about 0°C were measured, while during daytime about 8°C was reached at a cloudless sky; no wet deposition was reported. The mixing height, as measured by an

acoustic sounder increased from 175 m in the early morning to about 400 m in the afternoon.

The results for the PUFF model at 7.00, 10.00, 14.00 and 18.00 h are given in Fig. 7. The spatial average concentrations over The Netherlands are given for modelled and measured concentrations in Fig. 8. The correspondence is good; the differences between the PUFF and the GRID model, presented in the same figure are smaller than the differences between modelled and measured concentrations. The correlations between these quantities are given in Fig. 9; the PUFF model gives lower correlations especially before and during fumigation. These lower values are attributed rather to the emission inventory than to the relatively low degree of meteorological sophistication of the model.

In another case study with a south-westerly flow, not reported here, an almost constant correlation level of 0.7 was computed. The emission inventarisation will be updated by means of "remote sensing" gasburden measurements of SO_2 fluxes and by detailed analysis of modelled and measured concentrations. The measured and the modelled SO_2 concentrations in the 80 km square subarea for this case study are compared in Fig. 10. The measured concentration field depicts some irregular concentration maxima at the axis of the most dominant modelled plume, but due to the limited number of monitoring stations this plume is not properly reconstructed. The comparison illustrates the capability of the model for improvement of the interpretation of network measurement results.

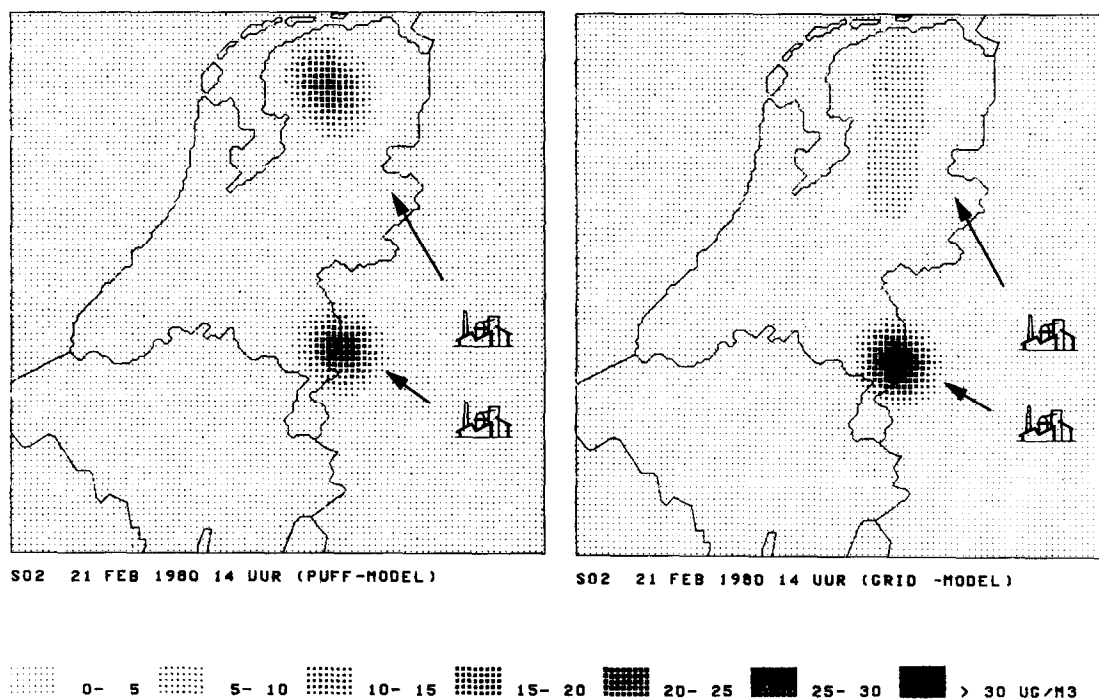


Fig. 6. SO_2 concentrations resulting from a high and a low source one hour emission puff, for both GRID and PUFF model.

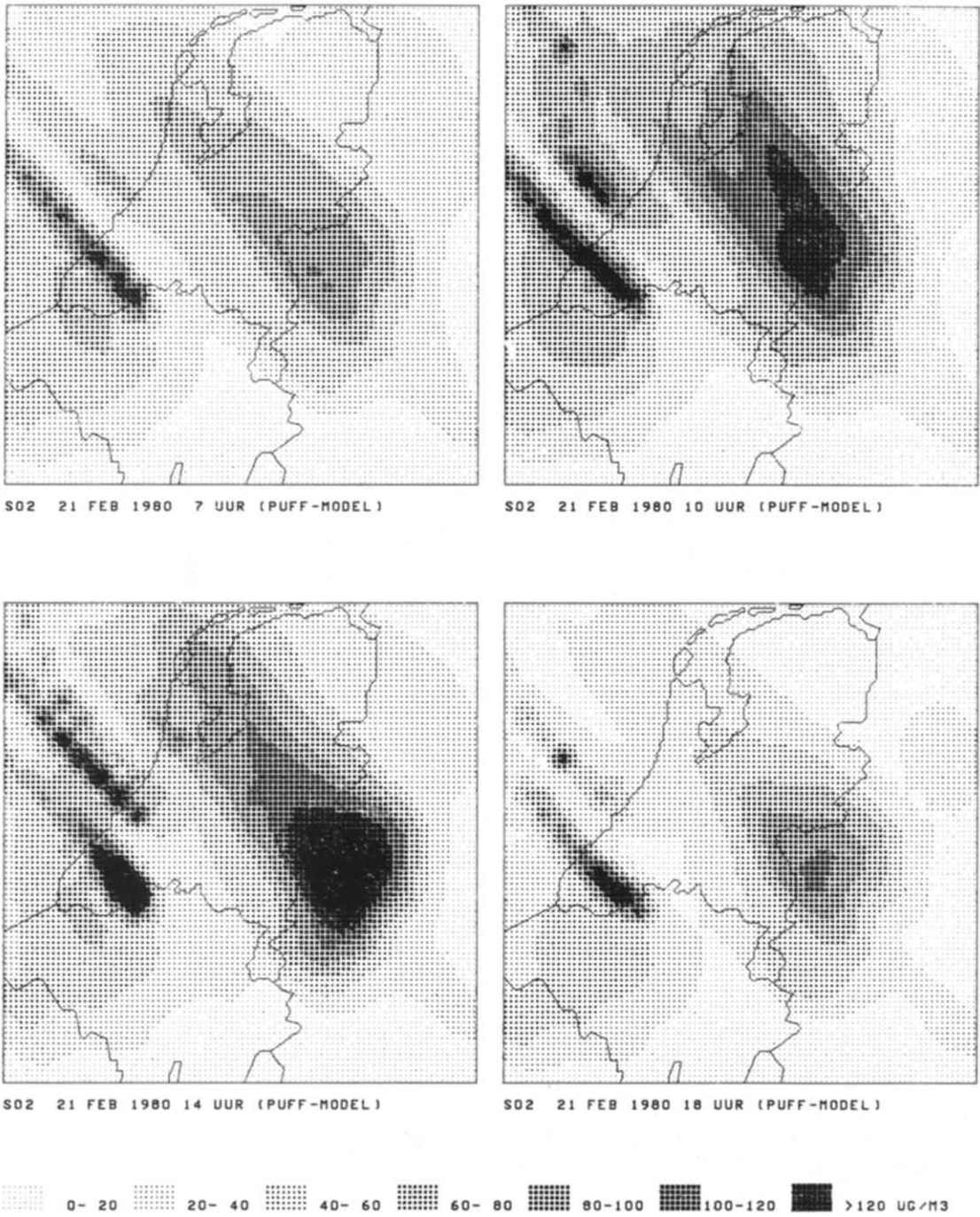


Fig. 7. SO₂ concentration fields in $\mu\text{g m}^{-3}$ as modelled by PUFF model at 21 February 1980.

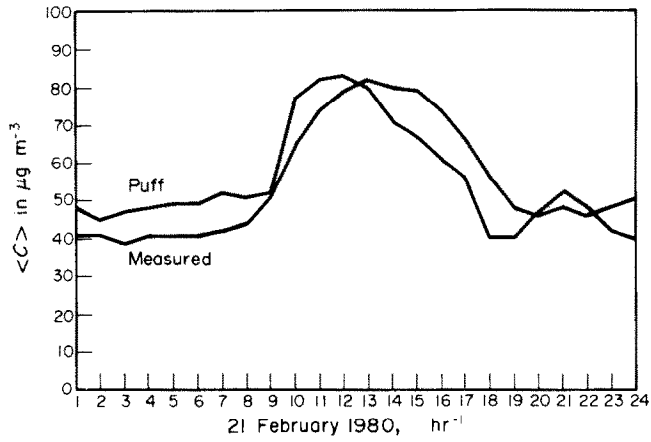


Fig. 8. Spatial average SO_2 concentrations in The Netherlands as measured and as modelled by the PUFF model; 21 February 1980.

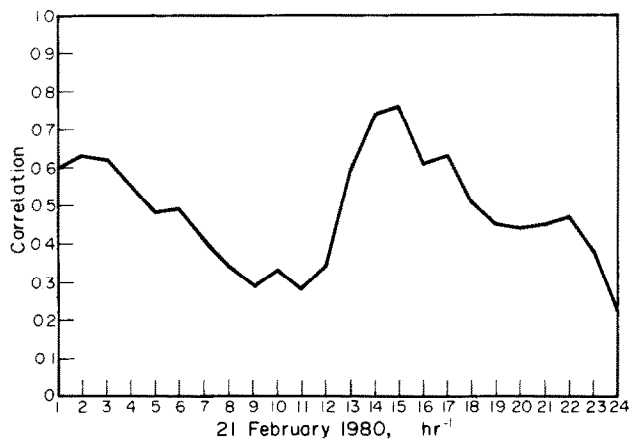
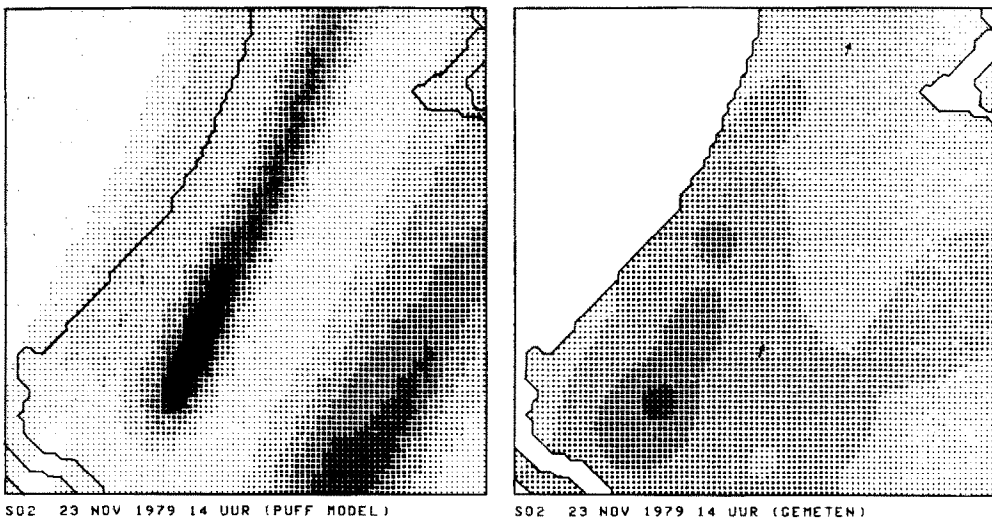


Fig. 9. Correlations between measured and modelled SO_2 concentrations; PUFF model.



0-50 50-100 100-150 150-200 200-250 250-300 >300 $\mu\text{g}/\text{m}^3$

Fig. 10. Modelled (left) and measured (right) SO_2 concentration field for the $80 \text{ km} \times 80 \text{ km}$ subarea of Holland; (23 November 1979, 14.00 h)

7. DISCUSSION AND CONCLUSION

The mesoscale PUFF model gives results comparable to the GRID type model, which is based on the same treatment of meteorology. The differences between the results of the two models mainly concern the improper treatment of wind shear dispersion in the PUFF model. However, this disadvantage is compensated by two features which are important for the intended operational applications:

(i) If the number of sources is smaller than 500, i.e. about 25% of the number of possible high and low sources in the GRID model ($2 \times 32 \times 32$ grids = 2048), the PUFF model has a higher computational efficiency than the GRID model at the same spatial resolution.

(ii) The PUFF model can evaluate extremely high spatial resolutions and consequently can be used for the combined interpretation of both local and remote contributions to the observed SO₂ levels.

These features make the PUFF model attractive for operational applications on mini- or even desk-top computers, to evaluate pollutant patterns for which first order chemistry can be assumed (SO₂, NO_x).

At a limited set of input parameters a reasonable model performance is achieved, as was demonstrated by a number of case studies. A selection of these case-studies for different weather types and wind directions, implying exchanges of SO₂ between The Netherlands, Belgium and Germany are presented by van Egmond (1982).

REFERENCES

- Csanady G. T. (1973) *Turbulent Diffusion in the Environment*. Reidel, Dordrecht, Holland.
- van Egmond N. D. and Kesseboom H. (1983) Mesoscale air pollution dispersion models—I. Eulerian GRID model. *Atmospheric Environment* 17, 257–265.
- van Egmond N. D. (1982) The study of mesoscale air pollution transport by routine applications of remote sensors. *Proc. 75th Annual Meeting of APCA*, Paper 82-631.
- Golder D. (1972) Relations among stability parameters in the surface layer. *Boundary-Layer Met.* 3, 47–58.
- TNO, Rekensysteem Luchtverontreiniging II (1979) TNO, Schoenmakerstraat, Delft, Netherlands.